Low-Density Polyethylene/Plasticized Tapioca Starch Blends with the Low-Density Polyethylene Functionalized with Maleate Ester: Mechanical and Thermal Properties

B. G. Girija, R. R. N. Sailaja

Department of Chemical Engineering, Indian Institute of Science, Bangalore 560012, India

Received 20 April 2004; accepted 6 December 2005
DOI 10.1002/app.24025
Published online in Wiley InterScience (www.interscience.wiley.com).

ABSTRACT: In this study, the mechanical and thermal properties of low-density polyethylene (LDPE)/thermoplastic tapioca starch blends were determined with LDPE-*g*-dibutyl maleate as the compatibilizer. Mechanical testing for the evaluation of the impact strength and tensile properties was carried our as per standard ASTM methods. Thermogravimetric analysis and differential scanning calorimetry were also used to assess the thermal degradation of the blends. Scanning electron micrographs were used to analyze fracture and blend morphologies. The results show significant improvement in the mechanical properties due to the addition of the compatibilizer, which effectively linked the two immiscible blend components. © 2006 Wiley Periodicals, Inc. J Appl Polym Sci 101: 1109–1120, 2006

Key words: LDPE; starch; compatibilizer; mechanical and thermal properties

INTRODUCTION

Low-density polyethylene (LDPE) has the largest tonnage in the world, and disposal of this plastic waste has become a major environmental hazard. Hence, attempts to develop biodegradable blends have been a focus of research for the past 4 decades. Fully biodegradable poly(hydroxyalkaonate)s have been developed, but they are very expensive compared to conventional plastic materials.[1] Another promising and cheaper alternative is a blend of LDPE with natural renewable aggroresources. This would also reduce our dependence on petroleum and mineral resources. Starch is such a renewable resource that is cheap and abundantly available. Otey and coworkers[2,3] blended starch with poly(ethylene-*co*-acrylic acid); this blend could be used for short-term packaging applications.

Starch powder when blended with thermoplastic degrades during processing. To facilitate processability, starch is treated with water and a glycerol plasticizer.[4] The mechanical properties of plasticized tapioca starch (TS)/LDPE are superior compared to granular starch/LDPE blends.

A major drawback in starch/LDPE blends is their incompatibility. Starch is a polar hydrophilic natural polymer, and LDPE is a nonpolar hydrophobic thermoplastic. To improve the interfacial adhesion between starch and LDPE, a compatibilizer, which is usually a functionalized polymer, has been used. Oxidized polyethylene (PE) was blended with starch by Jane et al.;[5] this led to enhanced tensile strength. A similar improvement in the mechanical properties was also obtained by Sailaja and coworkers[6,7] Maleic anhydride grafted LDPE has been used as the most common compatibilizer by a number of researchers[8–10] for improving the adhesion between LDPE and starch.

However, certain studies[11–13] have revealed that the grafting of maleate esters, such as dibutyl maleate (DBM) and diethyl maleate, are preferred over maleic anhydride. It has been suggested that DBM could be an alternative to maleic anhydride as a functionalizing agent, as the latter is very toxic and volatile and can strongly corrode the metallic equipment used in the melt process.[12] Studies on the grafting of DBM onto LDPE were carried out by Konar et al.[13] and, more recently, Rosales et al.[14] LDPE-*g*-DBM has been used to increase compatibility with magnesium hydroxide; this led to superior mechanical properties. The use of LDPE-*g*-DBM as a compatibilizer in LDPE/starch blends have not been investigated so far. In this study, the effect of the addition of this compatibilizer on the thermal and mechanical properties of LDPE/plasticized TS blends were examined.

EXPERIMENTAL

Materials

LDPE [grade 24FS040 with melt flow index of 4 g (10 min)$^{-1}$] from IPCL (Vadodara, India) was used for

Correspondence to: R. R. N. Sailaja (rrns@chemeng.iisc.ernet.in).

Journal of Applied Polymer Science, Vol. 101, 1109–1120 (2006)

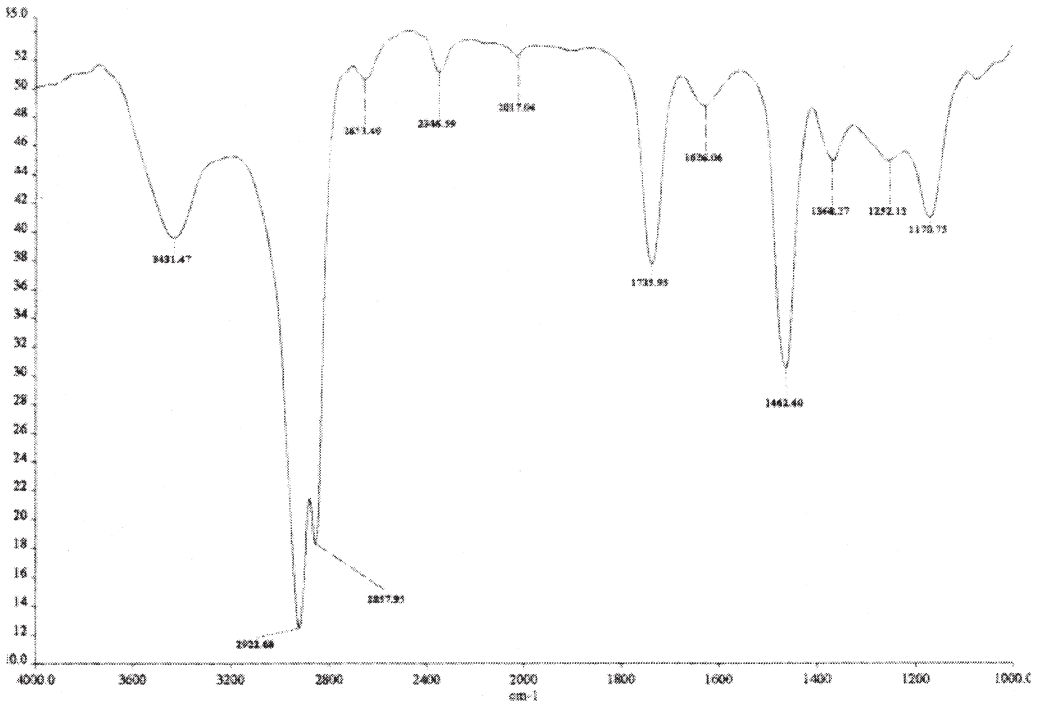

Figure 1 FTIR spectra of the LDPE-*g*-DBM compatibilizer.

blending with TS (particle size = 10.2 μm). The starch was obtained from tapioca plants grown in the South India state of Kerala. We prepared the plasticized TS by mixing 48% starch, 33% glycerol, and 19% water for 5 min and allowing the mixture to stand for 1 h. The mixture was then stirred for 30 min at 70°C. Iron stearate was used as an autooxidant. All of the other solvents and DBM were obtained from S. D. Fine Chemicals (Mumbai, India).

Synthesis of the compatibilizer

LDPE-*g*-DBM was prepared by the dissolution of LDPE in *O*-dichlorobenzene at 120°C; 0.2% of the dicumyl peroxide initiator was then added along with DBM. The reaction was carried out for 3 h at 120°C with continuous stirring. The product was cooled and precipitated in methanol and filtered. The grafted product was then washed several times with methanol and finally rinsed with acetone and dried. The product was characterized by Fourier transform infrared spectroscopy (FTIR), as shown in Figure 1. The stretching of the —C═O— bond could be clearly seen at 1750 cm^{-1}. The percentage grafting calculated as per Gonzalez et al.[15] was 2.2%

Melt blending

Blends of LDPE, TS, LDPE-*g*-DBM, and 0.1% iron stearate (autooxidant) were melt-mixed in various proportions at 210°C in air for 4 min in a heated cup fitted with a spiked motor. Before blending, the cup was thoroughly cleaned five times with pure LDPE. Dumbbell-shaped specimens were then molded into standard dies with a Minimax molder (Custom Scientific Instruments, NJ, model CS-183MMX). The amount of compatibilizer (*C*) was based on the weight percentage of TS in all cases throughout the study. The resulting blend was thermoplastic, as it could be remelted and remolded.

Mechanical properties of the blends

A Minimax impact tester (model CS-183T1079) and a tensile tester (model CS-183TTE; Custom Scientific Instruments, NJ) were used to measure the impact strength and tensile properties, respectively. At least eight specimens were tested for each variation in the composition of the blend. The impact and tensile tests were performed as per ASTM D 1822 and ASTM D 1708, respectively. The strain rate adapted for all tensile measurements was 10%/min.

Thermal analysis

Thermogravimetric analysis (TG) was carried out for the esterified starches and for the blends with a PerkinElmer Pyris Diamond 6000 analyzer (Perkin Elmer Inc., Shelton, CT) in a nitrogen atmosphere. The sample was subjected to a heating rate of 10°C/min in a heating range of 40–600°C with Al_2O_3 as the reference material. Differential scanning calorimetry (DSC)

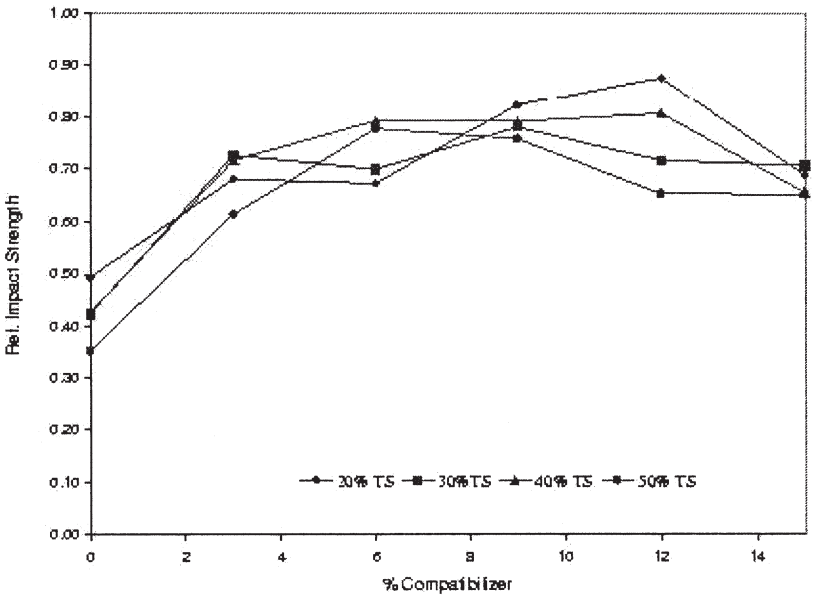

Figure 2 RIS of the percentage compatibilizer of the blends.

of the blend specimens was performed in a Mettler Toledo model DSC 822e instrument (Mettler Toledo AG, Switzerland). Samples were placed in sealed aluminum cells with a quantity of less than 10 mg and scanning at a heating rate of 10°C/min in a heating range of 25–200°C.

Blend morphology

Scanning electron microscopy (SEM; Jeol JSM-840 microscope) was used to study the morphology of the fractured and unfractured specimens. The specimens were gold sputtered before microcopy (Jeol, SM-1100E). The morphology of the unfractured blend specimens was taken after the samples were soaked for 24 h in water at 80°C.

RESULTS AND DISCUSSION

Blends of LDPE and TS were prepared with LDPE-*g*-DBM as a compatibilizer. The mechanical and thermal properties were measured for the blend specimens.

Relative impact strength (RIS)

The RIS (relative to LDPE) of the LDPE/TS blends are shown in Figure 2. A decrease in RIS was observed as TS loading increased and dropped to 0.35 at 50% TS loading. For 20 and 30% TS loading, the compatibilized blends attained RIS values of 0.9 and 0.8, respectively. For higher TS loadings, the impact strength values were almost 80% that of neat LDPE. The improvement in impact strength was mainly attributed to the improved adhesion between the filler and matrix due to the addition of the LDPE-*g*-DBM compatibilizer. For all TS loadings, the blends had an optimal impact strength around $C = 9$–12%, beyond which the values decreased. It was reported earlier[16] that above a certain compatibilizer loading, excess compatibilizer accumulates in one of the phases, and the system behaves like a ternary blend. To determine the quantitative relationship between response (Y), that is, RIS, and the system variables, that is, filler content (x_1) and weight percentage compatibilizer (x_2), the experimental data was fitted with the second-order quadratic equation given in eq. (1). The values of the coefficients (a_1–a_5) of the fitted equation for different mechanical properties (Y's) and $\langle r^2 \rangle$ values are given in Table I. The analysis of variance data was generated with sigma plot software (version 2):

$$x = a_0 + a_1x_1 + a_2c_2 + a_3{x_1}^2 + a_4{c_2}^2 + a_5x_1c_2 \quad (1)$$

The regression equation obtained for RIS values showed a very good fit with experiment data having a residual $\langle r^2 \rangle$ value of 0.85, as shown in Table I. The values of the coefficients are listed in Table I.

The SEM micrographs of the impact-fractured surfaces are shown in Figure 3. The fractured micrograph for 20% TS loading without compatibilizer showed large holes [Fig. 3(a)] due to the agglomeration of TS particles. TS is hydrophilic and polar, and LDPE is nonpolar and hydrophobic; this resulted in poor adhesion between the components in the blend. The matrix underwent deformation and crazing and resisted fracture to a certain extent. The addition of compatibilizer to this blend [Fig. 3(b)] showed ductile failure. Plastic deformation occurred during necking,

TABLE I
Coefficients for the Nonlinear Regression of Eq. (1)

	Linear terms			Quadratic terms		Interaction term:	Sum of squares	Residual	Standard error
Y	a_0	a_1	a_2	a_3	a_4	a_5	M	$\langle r^2 \rangle$	of estimate
RIS	0.4138	0.0767	0.0041	−0.0040	−0.0001	−0.00001	0.0694	0.85	0.0584
RTS	0.7971	0.0546	−0.0089	−0.0019	0.0001	−0.0001	0.1164	0.88	0.0651
RTM	1.0354	0.0651	−0.0133	−0.0047	0.0001	0.0007	0.1100	0.79	0.0931
REB	0.4367	0.0256	0.0061	−0.0018	−0.0001	0.0002	0.0188	0.85	0.0305
RW	0.4894	0.0394	−0.0069	−0.0014	0.0001	−0.0003	0.0393	0.86	0.0418

and voids were formed due to the debonding of filler particles, which gave rise to a rosette formation.[17] For 40% TS loading [Fig. 3(c)], profuse cavitation accompanied by matrix deformation was observed, which is typical of quasibrittle fracture. The fracture surface for the compatibilized blend [Fig. 3(d)] showed pulled-out regions of long and thick fibric bundles along with crazing and cavitation, which was not observed in the uncompatibilized blend. This was also reflected in the higher impact strength values for the compatibilized blend compared to uncompatibilized blends. The debonding of particles allowed the matrix to undergo large local strain and, thereby, resist fracture through an increase in the effective load-bearing area. We obtained similar results in our earlier work.[6,7]

Stress–strain curves

Figure 4 shows the engineering stress–strain curves for the LDPE/TS blends. For uncompatibilized blend with 20% TS loading [Fig. 4(a)], the curve showed the onset of craze formation after the yield point, and the specimen failed during neck propagation. Similar behavior was observed by Psomiadou et al.[18] for starch blends. The addition of 6% LDPE-*g*-DBM compatibilizer [Fig. 4(b)] to this blend created a marked improvement in the stress value accompanied by an increase in strain. This was due to good adhesion between the filler and matrix, which increased the load-bearing capacity of the blend specimen. The specimen showed onset of craze formation followed by crack nucleation, which caused fracture.[19] At higher TS loadings, poor strain values were observed due to weak adhesion [Fig. 4(c)] between the filler and matrix. The specimens failed during neck propagation,[16,17] which indicated quasibrittle fracture. The blend compatibilized with 6% LDPE-*g*-DBM showed significant improvement in strain values, which indicated increased ductility; the specimen failed during drawing and strain hardening [Fig. 4(d)].

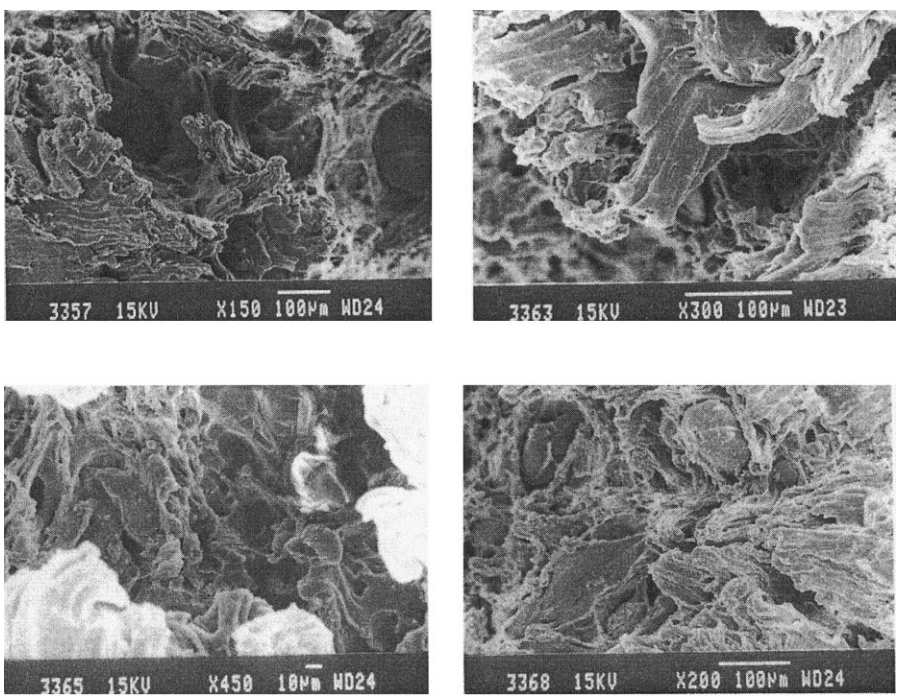

Figure 3 SEM micrographs of the impact-fractured blend specimens: (a) 20% TS and C = 0%, (b) 20% TS and C = 12%, (c) 40% TS and C = 0%, and (d) 40% TS and C = 12%.

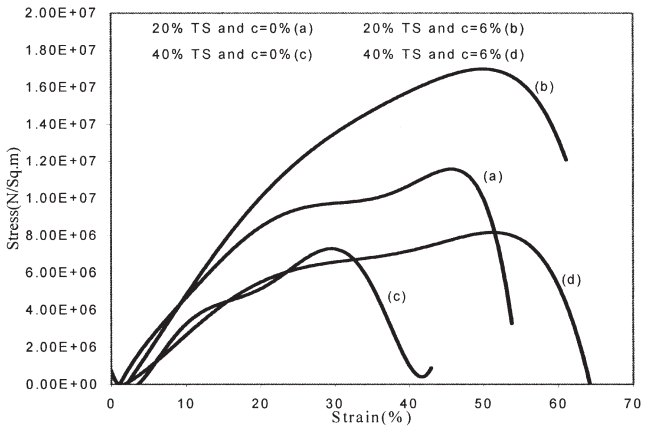

Figure 4 Engineering stress–strain curves for the LDPE/TS blends.

Relative work of rupture (RW)

The area under the stress–strain curve was the work of rupture and was a measure of the toughness of the blend. Figure 5 shows of plot of RW (the ratio of the work of rupture for the blend to the work of rupture for pure LDPE) versus *C*. For the 20% TS loading, the RW values increased from 0.35 (C = 0%) to 0.65 (C = 9%). For 30 and 40% TS loading, the RW values increased by 66% with a 12% compatibilized blend. However, for a still higher loading, that is, 50% RW values, the blends were only slightly improved by compatibilization. For 20–40% loading, the LDPE-*g*-DBM improved the dispersion between the polar hydrophilic starch and the nonpolar hydrophobic LDPE. However, for higher loadings of 50%, the matrix was able to resist fracture only to a certain extent, as there were too many weak links. The coefficients for the nonlinear regression are given in Table I. The equation gave an excellent fit with the experimental data with $\langle r^2 \rangle$ values greater than 0.8.

Relative tensile strength (RTS)

Figure 6 shows the effect of TS and compatibilizer loading on the RTS (relative to LDPE) of the blend. A decrease in the tensile strength values was observed with increasing TS loading from 20 to 50%. For 20 and 30% loading, the tensile strength increased drastically and was same as that of the unfilled LDPE. For higher loadings, 40 and 50%, the RTS values increased significantly and were around 75% of that of neat LDPE. The high tensile strength values for the compatibilized blends indicated good adhesion and stress transfer from the matrix to the filler. The PE-*g*-DBM may have possibly undergone reactive blending with the starch hydroxyl groups, as shown in Scheme 1. The nonlinear regression coefficients are given in Table I.

Two theoretical models were used to predict tensile strength and compare them with the experimental data. Nicolais and Narkis[20] proposed the following equation for calculating the tensile strength of blends (σ_b):

$$\mathrm{RTS} = \frac{\sigma_b}{\sigma_{\mathrm{LDPE}}} = 1 - 1.21\phi_f^{2/3} \tag{2}$$

where σ_{LDPE} is the tensile strength of neat LDPE and ϕ_f is the volume fraction of the filler, that is, TS. The volume fractions (ϕ_i's) were calculated, as suggested by Willett,[20] with eq. (3):

$$\phi_i = \frac{W_i/\rho_i}{\sum W_i/\rho_i} \tag{3}$$

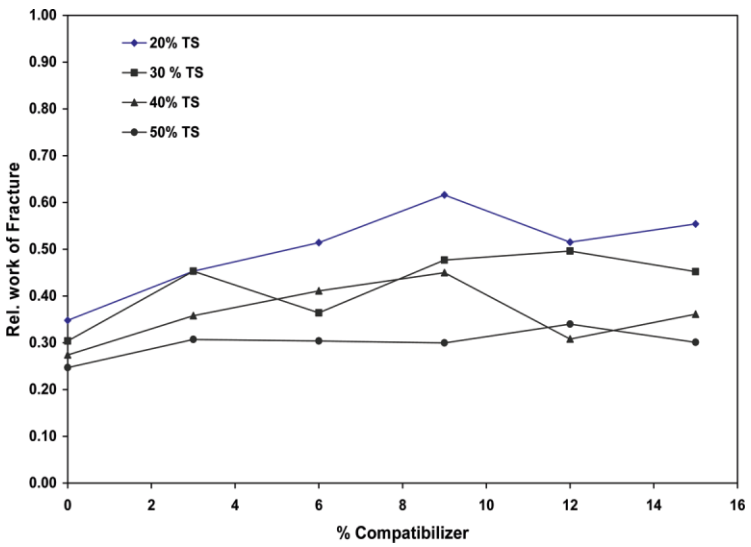

Figure 5 Blend RW values versus percentage compatibilizer. [Color figure can be viewed in the online issue, which is available at www.interscience.wiley.com.]

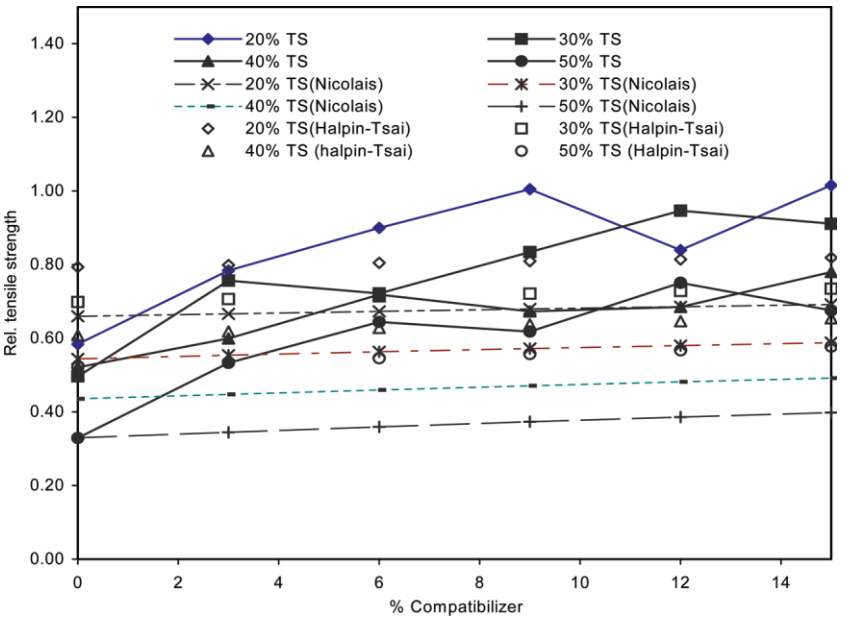

Figure 6 RTS versus percentage compatibilizer. [Color figure can be viewed in the online issue, which is available at www.interscience.wiley.com.]

where ρ_i and W_i are the density and weight fraction, respectively, of component i in the blend. The density values of LDPE were taken to be 0.93 g/cm^3, whereas that for TS was measured to be 1.395 g/cm^3, respectively. The calculated values from eq. (2) are also plotted in Figure 6. The experimental data agreed well with the theoretical data for our compatibilized blends. For compatibilized blends, the theoretical values were lower than the measured tensile strength values. This was due to the fact that the model assumes poor bonding between the matrix and the filler,[21] which results in little stress transfer from the matrix to the filler. The agreement with the model for the uncompatibilized blends indicated weak adhesion between the filler and the matrix. For compatibilized blends, the experimental values were much higher, which indicated good adhesion and subsequently efficient stress transfer leading to enhanced tensile strength values.

Earlier work done by Sailaja and Chanda[8] with LDPE-*g*-maleic anhydride as a compatibilizer did not show any marked improvement in the tensile strength values. The use of other functionalized PEs as compatibilizers by Sailaja and coworkers[6,7] similarly did not show much improvement in RTS.

The other model fitted was the Halpin–Tsai model[20] given in eq. (4):

$$\mathrm{RTS} = \frac{\sigma b}{\sigma \mathrm{LDPE}} = \frac{1 + G\eta_T\phi}{1 - \eta_T\phi} \tag{4}$$

where variable η_T is given by

$$\eta_T = \frac{R_T - 1}{R_T + G} \tag{5}$$

where R_T is the ratio of the filler tensile strength to the tensile strength of the LDPE matrix (unfilled). The constant G is given by eq. (6) as follows:

$$G = \frac{7 - 5\nu}{8 - 10\nu} \tag{6}$$

where ν is Poisson's ratio of LDPE and was taken to be 0.43.[20] R_T was calculated to match the experimental data and was found to be 0.45. For the uncompatibilized blends, the Halpin–Tsai model failed because of poor adhesion. However, for the compatibilized blends, the experimental data was close to the pre-

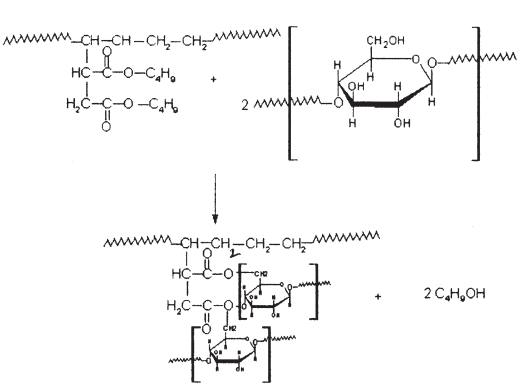

Scheme 1

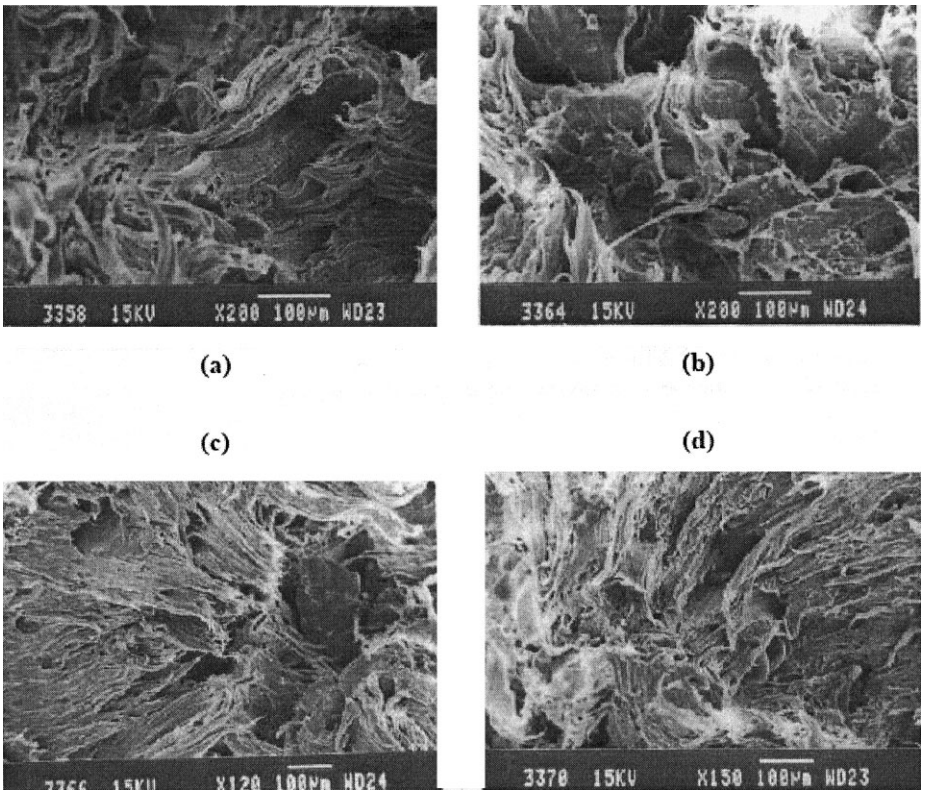

Figure 7 SEM micrographs for the tensile-fractured blend specimens: (a) 20% TS and $C = 0\%$, (b) 20% TS and $C = 12\%$, (c) 40% TS and $C = 0\%$, and (d) 40% TS and $C = 12\%$.

dicted value due to improved interfacial adhesion, as shown in Figure 6.

The SEM micrographs for tensile fracture for the compatibilized and uncompatibilized blend specimens are shown in Figure 7. For 20% TS content, the material underwent failure due to crazing, cavitation, and shearing of the matrix into thin fibril bundles [Fig. 7(a)], even for the uncompatibilized blend. The matrix was able to withstand the load because starch content was low. The addition of compatibilizer showed a similar mode of failure [Fig. 7(b)], except that the sheared fibril bundles were thicker. For a higher TS loading of 40%, large plastic deformation, crazing, and voiding due to the debonding of agglomerated filler particles were observed (no LDPE-*g*-DBM). For the compatibilized blends, extensive fibrillation, rosette formation, and cavitation leading to small voids were observed [Fig. 7(d)] due to improved dispersion. This was also reflected in the improvement of tensile strength values (Fig. 6) for the compatibilized blend.

Relative tensile modulus (RYM)

Figure 8 shows RYM of the TS/LDPE blends with LDPE-*g*-DBM as a compatibilizer. RYM was the ratio of the tensile modulus of the blend (E_b) to the tensile modulus of the unfilled LDPE (E_{LDPE}). RYM values decreased as TS loading increased due to the plasticizing effect of glycerol; for compatibilized (9–12%) blends with 20–50% TS exhibited modulus values that were the same as that of unfilled LDPE with 9–12% LDPE-*g*-DBM. Thus, the compatibilizer linked TS effectively with LDPE and improved the dispersion of TS in the matrix. The nonlinear regression coefficients for eq. (1) with respect to the property of RYM are given in Table I. Earlier work done by Sailaja and coworkers[6–8] showed significant improvement in the RYM values of around 0.8 with other compatibilizers, including LDPE-*g*-maleic anhydride, epoxy-functionalized LDPE, and ethylene–vinyl alcohol copolymer. PE-*g*-DBM compatibilizer showed a similar improvement in RYM with values equal to 1.0, the same as LDPE.

Kerner's model[20] was used to predict the theoretical values for this blend with the following equation:

$$\mathrm{RYM} = \frac{E_b}{E_{\mathrm{LDPE}}} = \left[1 + \left(\frac{\phi_f}{1 - \phi_f}\right)\left(\frac{15(1 - \nu)}{(8 - 10\nu)}\right)\right] \quad (7)$$

The values calculated with eq. (7) did not match the obtained experimental data. It was obvious as this model does not consider interaction between the filler and matrix. However, strong interactions can cause a stiffening effect on the polymer matrix adjacent to

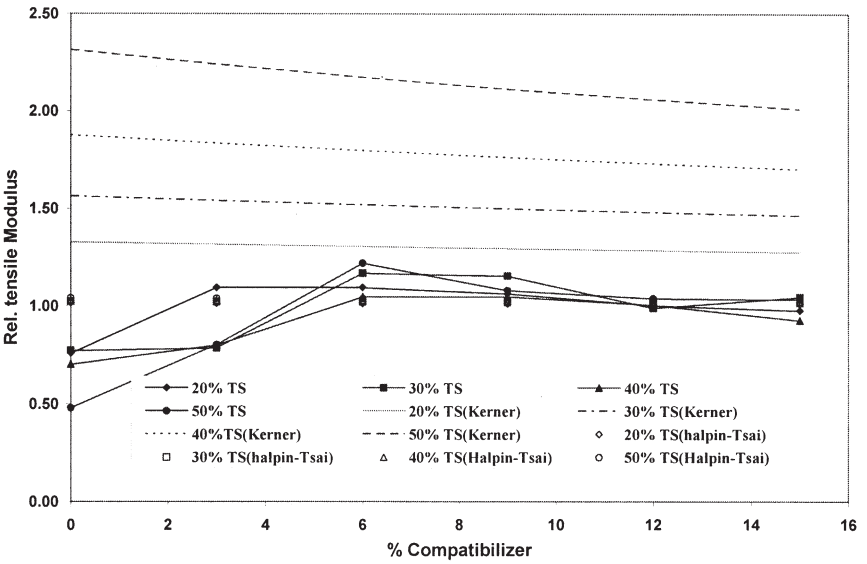

Figure 8 Blend RYM values versus percentage compatibilizer.

filler particles.[22] The other model was the Halpin–Tsai model, whose equation for RYM is given as follows:

$$\mathrm{RYM} = \frac{E_b}{E_{\mathrm{LDPE}}} = \left(\frac{1 + G\eta\phi_f}{1 - \eta\phi_f}\right) \tag{8}$$

where $\eta = (R - 1/R + G)$, $G = (7\text{–}5\nu/8\text{–}10\nu)$, where R is the ratio of the filler modulus to the matrix modulus. The value of R found by trial and error was found to be 1.6. The uncompatibilized blends did not agree well with the values calculated by the Halpin–Tsai model due to weak adhesion. For compatibilized blends, the values agreed very well with the predicted data (Fig. 8).

Relative elongation at break (REB)

Figure 9 shows a plot of REB, that is, the ratio of the elongation at break for the blend (ε_b) to the elongation at break for pure LDPE ($\varepsilon_{\mathrm{LDPE}}$). ε_b decreased as the TS loading increased due to poor adhesion between the polar filler and the nonpolar matrix. For 20–40% loading of TS in blends, the REB values improved with the addition of compatibilizer. For 50% TS loading, the REB values were 53% of that of pure LDPE for the compatibilized blends. The coefficients for eq. (1) are given in Table I.

Earlier work carried out by Sailaja and coworkers,[6–8] however, showed a significant improvement in

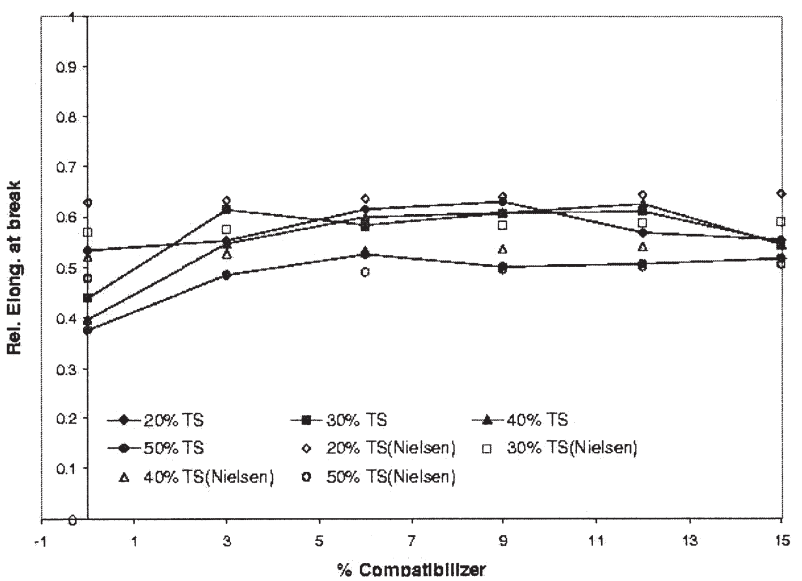

Figure 9 Blend REB values versus percentage compatibilizer.

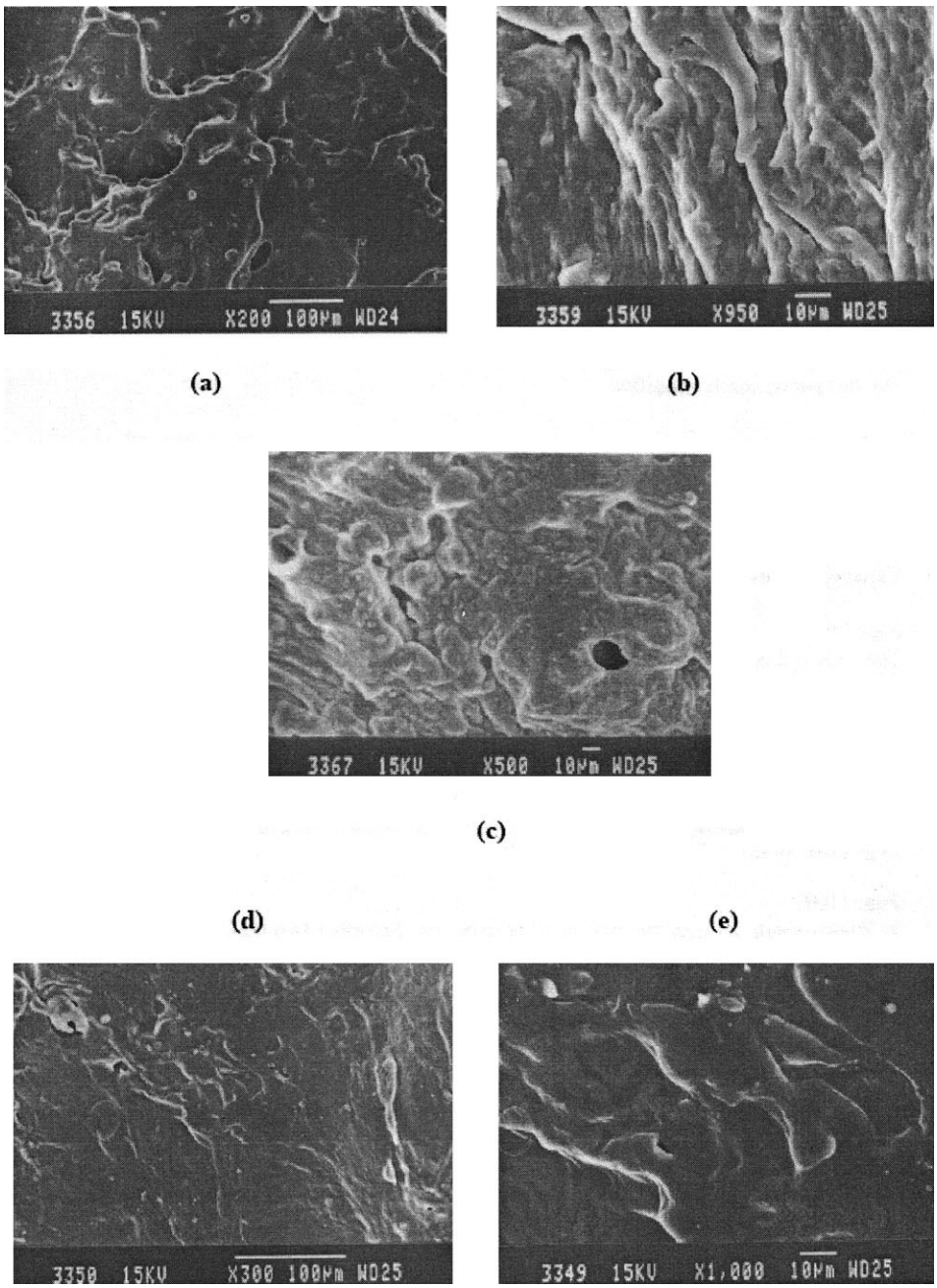

Figure 10 SEM micrographs showing the blend morphology of the blend specimens: (a) 20% TS and $C = 0\%$, (b) 20% TS and $C = 12\%$, (c) 40% TS and $C = 12\%$, (d) 50% TS and $C = 15\%$, and (e) 50% TS and $C = 15\%$ at a higher magnification than SEM micrograph d.

REB values through the addition of compatibilizers, which approached values close to that of LDPE, that is, REB values close to 1. PE-*g*-DBM showed an improvement in REB values compared to uncompatibilized blends but had a value around 0.7%, that is, 70% of that of LDPE for 20–40% TS loading.

The Nielsen's model[23] for REB is given by

$$\text{REB} = \frac{\varepsilon_b}{\varepsilon_{\text{LDPE}}} = (1 - k\phi_f^{1/3}) \tag{9}$$

where k is an adjustable parameter depending on filler geometry. The k value was 0.8, which was close to that found by Isabelle et al.[23] The theoretical values obtained for the uncompatibilized blends were higher than the experimental values. For the compatibilized blends, the predicted values were very close to the experimental data. The discrepancies between the theoretical and experimental values arose because of the assumption made for the Nielsen's model. In this model, the filler particles are cubic in shape, that is, k

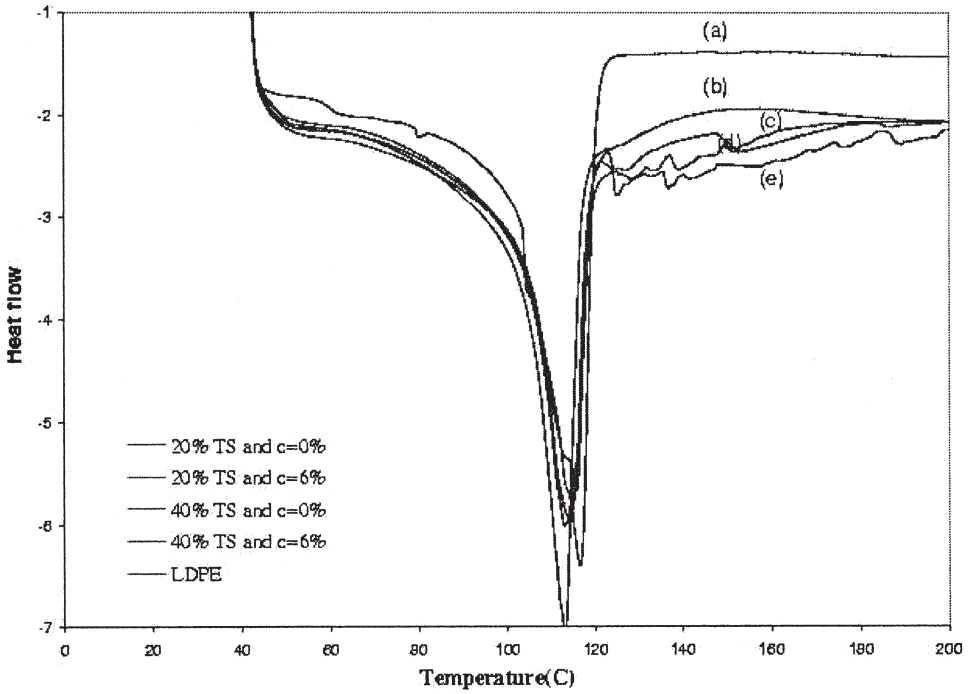

Figure 11 DSC thermograms for the LDPE/TS blends.

= 1, which was not the case. Perfect adhesion between the two phases is also assumed, which is usually not so. The deviations for the uncompatibilized blends were high, which indicated poor adhesion. For the compatibilized blends, the deviation from the predicted value was much less because of improved interfacial adhesion, but the values were lower than the calculated theoretical values.

Blend morphology

The morphology of the blend specimens is shown in Figure 10. The blend specimens were soaked for 24 h in water at 80°C. The uncompatibilized blend showed neat holes [Fig. 10(a)] left by starch particles during etching due to poor adhesion. The compatibilized blend showed a coarse surface and interlocking of TS particles with LDPE [Fig. 10(b)], thereby offering resistance to the debonding of TS particles. For the compatibilized blend with a 40% TS loading [Fig. 10(c)], a similar surface with protruded voids created by the etched TS particles indicated good interaction between TS and LDPE. For still higher, that is, 50%, TS loading (compatibilizer), the two phases were indistinguishable [Fig. 10(d)]. The same micrograph, when viewed at a higher magnification [Fig. 10(e)], showed a coarse interlocked surface similar to that shown in Figure 10(b). A similar observation was made by Murata and Anazewa[24] and Jiang et al.[25] for etched blend specimens. They suggested that efficient compatibilization leads to such a bicontinuous structure in which one phase is wrapped in the other. Further, it was observed that there exists some extent of adhesion for LDPE/TS blends.[26] It was argued that the compression exerted by a crystalline matrix on an amorphous dispersed phase could result in good interfacial contact. This could be the reason for the coarse morphology and resistance to fracture for the blend specimens even without the addition of compatibilizer. A functionalized polymer as a compatibilizer, therefore, further enhances the interfacial linkage between the blend components.

DSC analysis

Figure 11 shows the DSC thermograms for the LDPE/TS blends. The thermal analysis at a heating rate of 10°C/min was carried out in the temperature range 25–200°C. The heat of fusion (ΔH_f) for the samples was determined by the calculation of the area under the peaks. The percentage crystallinity (X_c) of the LDPE phase was determined with the following equation:

$$X_c = \frac{\Delta H_f}{\Delta H_f^0} \times 100 \qquad (10)$$

where ΔH_f^0 is the heat of fusion for the 100% crystalline LDPE and was taken to be 287.6 J/g.[27] The onset temperature (T_0) and melting endset temperature (T_E), along with the calculated X_c values, are given in Table II. There was not much difference in the melting temperatures for

TABLE II
DSC Analysis for the TS/LDPE Blends

Blend composition	T_0 (K)	Peak temperature (K)	T_E (K)	X_c
LDPE	337.764	385.27	398.27	33.740
20% TS and $C = 0$	375.57	386.19	390.45	29.976
20% TS and $C = 6$	377.29	386.23	392.19	20.384
40% TS and $C = 0$	377.24	387.23	391.69	17.342
40% TS and $C = 6$	375.18	388.91	392.09	16.218
50% TS and $C = 12$	375.00	385.30	390.21	12.057

the blends. The crystallinity, however, decreased as TS loading increased. This may have been due to the incorporation of TS in the blends, which inhibited close packing of the LDPE chains. For compatibilized blends, the crystallinity was still reduced compared to that of the uncompatibilized blends. This indicated strong interactions between the blend components.

TGA

Figure 12(a,b) shows the thermogravimetric analysis (TG) versus temperature plots for LDPE/TS blends with and without compatibilizer. The curves for pure TS and pure LDPE are also shown in Figure 12 for the sake of comparison. The plasticized starch showed a

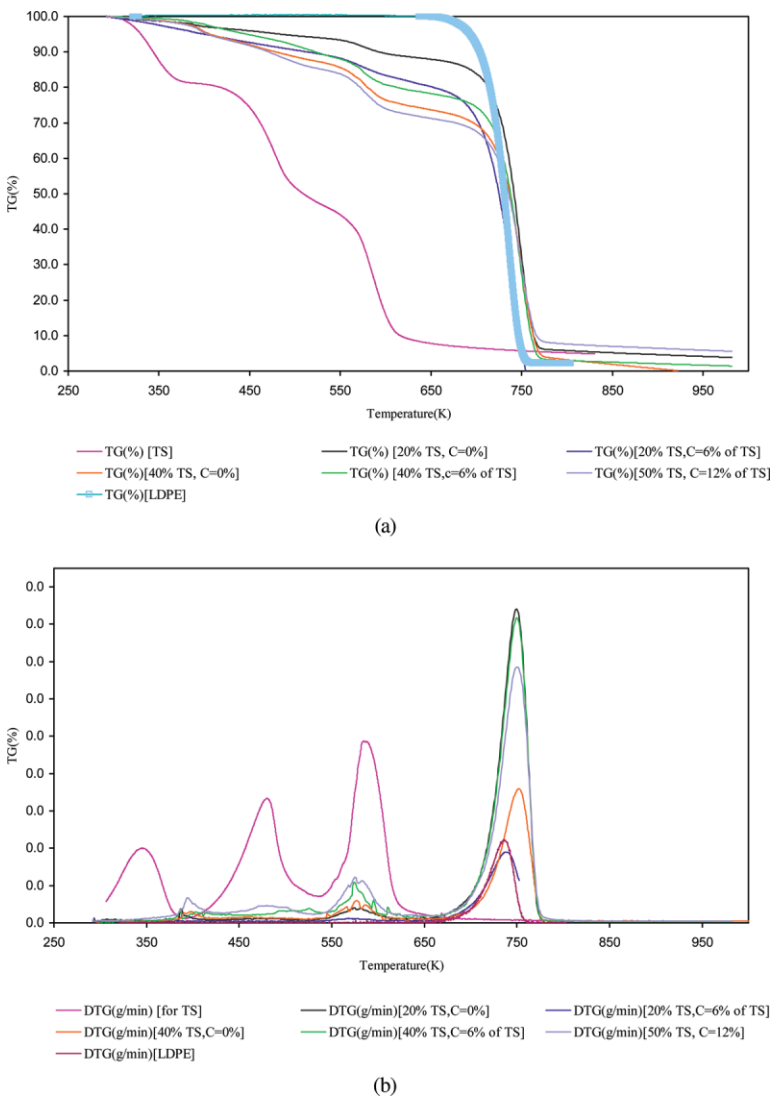

Figure 12 (a) TGA and (b) DTG thermograms for the LDPE/TS blends. [Color figure can be viewed in the online issue, which is available at www.interscience.wiley.com.]

three-stage degradation. The first peak at 350 K was due to water evaporation. The second peak at 482 K was due to the loss of the glycerol plasticizer. The third peak at 591 K was attributed to the thermal degradation of starch. At this temperature, thermal condensation between hydroxyl groups forming ether links and ring scission of glucoside units took place.[28] For pure LDPE, the peak at 740 K due to the decomposition of the C—C backbone led to an 80% weight loss. The addition of 20% TS to LDPE with no compatibilizer showed two main peaks at 584 K, due to starch degradation, and 751 K, with a 72% weight loss due to LDPE degradation. For the compatibilized blend (6% PE-*g*-DBM), a similar two-stage degradation was observed, but the peaks were slightly shifted to lower temperature at 576 and 741 K for starch and LDPE degradation, respectively. The shifts to lower temperatures in the blend indicated some interactions between the blend components. A similar trend was observed for blends with 40% TS loading, as shown in Figure 12. Thermal degradation is a crucial aspect, as it affects the extent of degradation and the maximum temperature used in blend processing. The DTG curves with peaks are shown as Figure 12(b). Thermal analysis is crucial in the determination of the maximum temperature used during blend processing and, thereby, assesses the quality of the blend.

CONCLUSIONS

The mechanical and thermal properties of LDPE/TS blends were investigated with LDPE-*g*-DBM as a compatibilizer. The plasticization of starch with glycerol and water eased the processability of the starch. The compatibilizer improved the interfacial adhesion between the hydrophilic TS and hydrophobic LDPE. This improved the dispersion of TS in the LDPE matrix and thereby efficient stress transfer from the matrix to the particles. These resulted in enhanced mechanical properties compared to uncompatibilized blends, especially in impact strength, tensile strength, and tensile modulus values, which approached those of neat LDPE. Thermal studies with TG revealed the temperature for maximum loss. The thermal stability of the blends decreased with increased filler loading. DSC studies revealed a loss of crystallinity as the TS loading was increased.

References

1. Chanda, M.; Roy, S. K. Plastics Technology Handbook; Marcel Dekker: New York, 1998; p 1024.
2. Otey, F. H.; Westhoff, R. P.; Russell, C. R. Ind Eng Chem Prod Res Dev 1977, 16, 305.
3. Otey, F. H.; Westhoff, R. P. Ind Eng Chem Prod Res Dev 1984, 23, 284.
4. St-Pierre, N.; Favis, B. D.; Ramsay, B. A.; Ramsay, J. A.; Verhoogt, H. Polymer 1997, 38, 647.
5. Jane, J.; Gelina, R. J.; Nikolov, Z. L.; Evangelista, R. L. U.S. Pat. 5,059,642 (1991).
6. Sailaja, R. R. N.; Chanda, M. J Appl Polym Sci 2002, 86, 3126.
7. Sailaja, R. R. N.; Prasad Reddy, A.; Chanda, M. Polym Int 2001, 50, 1352.
8. Sailaja, R. R. N.; Chanda, M. J Polym Mater 2000, 17, 165.
9. Bikiaris, D.; Prinos, J.; Koustopoulos, K.; Pavlidou, E.; Frangis, N.; Panayiotou, C. Polym Degrad Stab 59, 287, 1998.
10. Bikiaris, D.; Panayiotou, C. J Appl Polym Sci 1998, 70, 1503.
11. Moad, G. Prog Polym Sci 1999, 24, 81.
12. Wang, Z.; Qu, B.; Fan, W.; Hu, Y.; Shen, X. Polym Degrad Stab 2002, 76, 123.
13. Konar, J.; Sen, A. K.; Bhowmick, A. K. J Appl Polym Sci 1993, 48, 1579.
14. Rosales, C.; Marquez, L.; Perera, R.; Rojas, H. Eur Polym J 2003, 39, 1899.
15. Rosales, C.; Perera, R.; Ichazo, M.; Gonzalez, R. J Appl Polym Sci 1998, 70, 161.
16. Sundararaj, U.; Macosko, C. W. Macromolecules 1995, 28, 2647.
17. Bazhenov, S.; Li, J. X.; Hiltner, A.; Baer, E. J Appl Polym Sci 1994, 52, 243.
18. Psomiadou, E.; Arvannitoyannis, I.; Biliaderis, C. G.; Ogawa, H.; Kawasaki, N. Carbohydr Polym 1997, 33, 227.
19. Li, J. X.; Hiltner, A.; Baer, E. J Appl Polym Sci 1994, 52, 269.
20. Willett, J. L. J Appl Polym Sci 1994, 54, 1685.
21. Lundquist, L.; Marque, B.; Hagstrand, P. O.; Leterrier, Y.; Manson, J. A. E. Compos Sci Technol 2003, 63, 137.
22. Shang, S. W.; Williams, J. W.; Soderholm, K. J Mater Sci 1994, 29, 2406.
23. Isabelle, F.; Micheline, B.; Alain, M. Polymer 1998, 39, 4773.
24. Murata, K.; Anazewa, T. Polymer 2002, 43, 6575.
25. Jiang, C.; Filipi, S.; Magagnini, P. Polymer 2003, 44, 2411.
26. Rodriguez-Gonzalez, F. J.; Ramsay, B. A.; Favis, B. D. Polymer 2003, 44, 1517.
27. Hatakeyama, T.; Liu, Z. Handbook of Thermal Analysis; Wiley: New York, 1999.
28. Mano, J. F.; Koiarova, D.; Reis, R. L. J Mater Sci Mater Med 2003, 14, 127.